Thermal charm production in a quark-gluon plasma in Pb-Pb collisions at $\sqrt{s_{NN}} = 5.5$ TeV

Ben-Wei Zhang,* Che Ming Ko, and Wei Liu
Cyclotron Institute and Physics Department, Texas A&M University, College Station, Texas 77843-3366, USA
(Received 25 September 2007; published 5 February 2008)

Charm production from the quark-gluon plasma created in the midrapidity of central heavy ion collisions at the Large Hadron Collider (LHC) is studied in the next-to-leading order in QCD. Using a schematic longitudinally boost-invariant and transversally expanding fire-cylinder model, we find that charm production could be appreciably enhanced at LHC as a result of the high temperature that is expected to be reached in the produced quark-gluon plasma. Sensitivities of our results to the number of charm quark pairs produced from initial hard scattering, the initial thermalization time and temperature of the quark-gluon plasma, and the charm quark mass are also studied.

DOI: 10.1103/PhysRevC.77.024901 PACS number(s): 24.85.+p, 25.75.−q, 12.38.Mh

I. INTRODUCTION

In heavy ion collisions at relativistic energies, hadrons composed of confined quarks and gluons are expected to dissolve into their constituents and form an extended volume of quark-gluon plasma (QGP). Experiments at the Relativistic Heavy Ion Collider (RHIC) have indeed shown that the results are consistent with the formation of a strongly interacting quark-gluon plasma during the initial stage of the collisions [1–4]. Many observables have been proposed to probe the properties of the quark-gluon plasma. Among them is the production of particles consisting of heavy charm and bottom quarks. In particular, it has been suggested that the production of charmonium J/ψ in relativistic heavy ion collisions might be suppressed as a result of its dissociation in the produced quark-gluon plasma due to the Debye screening [5]. Although recent studies based on the lattice QCD have indicated that the J/ψ can survive in the quark-gluon plasma at temperatures up to about twice the deconfinement temperature [6,7], J/ψ production in relativistic heavy ion collisions may still be suppressed in heavy ion collisions at RHIC [8–10]. However, if the initial produced charm quark pairs are large, such as in heavy ion collisions at Large Hadron Collider (LHC), J/ψ production could be enhanced through regeneration from charm and anticharm quarks in the quark-gluon plasma [11] as well as through statistical production from [12] or coalescence of [13] charm and anticharm quarks during hadronization of the quark-gluon plasma. These mechanisms for J/ψ production would become even more important if there are other sources for charm quark production in relativistic heavy ion collisions. To use charmonium and bottomonium production in relativistic heavy ion collisions as a diagnostic tool for the properties of produced quark-gluon plasma [9–12], it is thus essential to understand the production mechanism of charm and bottom quarks in these collisions.

In heavy ion collisions, there are generally four different contributions to charm production: direct and prethermal production from partonic interactions as well as thermal production from partonic and hadronic interactions. The direct production is from initial hard scatterings of partons in the nucleons from the colliding nuclei, which happens at a time scale of about $1/m_c \sim 0.15\,\mathrm{fm}/c$, with m_c being the charm quark mass. It contributes about three charm quark pairs in one unit of midrapidity in Au + Au collisions at $\sqrt{s_{NN}} = 200$ GeV at RHIC, and this number is increased to about 20 in Pb + Pb collisions at $\sqrt{s_{NN}} = 5.5$ TeV at LHC [14,15]. These numbers have, however, substantial uncertainty, particularly in extrapolating to LHC energy from that at RHIC [12,14], where measurements from PHENIX for p + p collisions [16] and STAR for d + Au collisions [17] disagree by about a factor of 2. The prethermal production is from produced partonic matter before it reaches thermal equilibrium. Based on consideration of minijet partons, it has been shown in Ref. [18] that this contribution is unimportant compared to that from direct production. For thermal production, it can be from the thermalized partonic matter or quark-gluon plasma as well as from the hadronic matter formed after the hadronization of the quark-gluon plasma. For thermal production of charm quark pairs from the quark-gluon plasma, studies so far have been based on the lowest-order QCD process of gluon-gluon fusion. The results show that its contribution depends sensitively on the initial temperature of produced quark-gluon plasma [19–23] and could be important if the initial temperature is high. In hadronic matter, charmed hadron can be produced from reactions such as $\pi N \to D\Lambda_c$ [24], $\rho N \to D\Lambda_c$ [25], and $NN \to N\Lambda_c D$ [26]. According to Ref. [27] based on Hadron-String Dynamics (HSD) without a partonic stage, secondary meson-baryon reactions in the hadronic matter give rise to approximately 11% enhancement of charm pair production in heavy ion collisions at RHIC energies. This contribution is, however, expected to be much smaller if one takes into account the formation of the quark-gluon plasma in the collisions, which would lead to a final hadronic matter with density and temperature significantly lower than those in the HSD model.

For Au + Au collisions at $\sqrt{s_{NN}} = 200$ GeV at RHIC, charm production is dominated by direct production as the contribution from thermal production is negligible due to the relatively low initial temperature (∼350 MeV) of produced quark-gluon plasma. Because the thermal production rate

*On leave from Institute of Particle Physics, Central China Normal University, Wuhan 430079, China.

increases exponentially with temperature as we show later, thermal production of charm quark pairs in Pb + Pb collisions at $\sqrt{s_{NN}} = 5.5$ TeV at LHC, in which a quark-gluon plasma with initial temperature and density much higher than those at RHIC is expected to be created, will be greatly enhanced. On the other hand, charm production from initial hard scattering of colliding nucleons increases only logarithmically with the collision energy. In most studies on the production of charm particles at LHC, it has been assumed, however, that thermal production can be neglected as well, and only the direct production from initial hard scattering has been considered. In the present study, we consider thermal charm production at LHC and compare its contribution to that due to direct production to see whether this assumption can be justified or under what conditions it can be considered as a good approximation.

Charm production in a quark-gluon plasma has been previously studied in the lowest-order QCD [19–22,28,29]. In our study, we consider thermal charm production in the next-to-leading order and investigate its sensitivity to the initial conditions of the produced quark-gluon plasma at LHC. We find that based on a reasonable estimation of the initial conditions, thermal charm production could play an important role in determining the total number of charm pairs produced in relativistic heavy ion collisions.

This article is organized as follows. In the next section, we discuss the processes and corresponding cross sections for thermal charm production in the leading order as well as the next-to-leading order in QCD. In Sec. III, we introduce the time evolution of formed quark-gluon plasma in heavy ion collisions at LHC and derive the rate equation for charm production in the quark-gluon plasma. In Sec. IV, we present the numerical results on thermal charm production at LHC and their dependence on the initial conditions and other parameters in the model. Finally, a summary and conclusions are given in Sec. V.

II. CHARM PRODUCTION FROM QUARK AND GLUON INTERACTIONS

A. Charm production cross sections

Previous studies of thermal charm production in a quark-gluon plasma [19–23] were all based on the following leading-order processes in QCD:

$$q + \bar{q} \to c + \bar{c}, \tag{1}$$

$$g + g \to c + \bar{c}. \tag{2}$$

In the present study, we include also the next-order $2 \to 3$ processes

$$q + \bar{q} \to c + \bar{c} + g, \tag{3}$$

$$g + g \to c + \bar{c} + g, \tag{4}$$

and the interferences between the leading-order processes with their virtual corrections due to vertex corrections and self energy insertions as their contributions are of the same order in the QCD coupling as the next-order $2 \to 3$ processes. We neglect, however, next-order $2 \to 3$ processes involving the gluon-quark interactions

$$\begin{aligned} g + q &\to c + \bar{c} + q, \\ g + \bar{q} &\to c + \bar{c} + \bar{q}, \end{aligned} \tag{5}$$

as their contributions are less important compared to other processes, especially the gluon-gluon fusion process of Eq. (4). This is largely due to the smaller color factor from the gluon-quark interaction vertex as compared to that from the gluon-gluon vertex and the fact that the charm pair can be produced from two incoming gluon lines in gluon-gluon fusion process, whereas in the gluon-quark process it can only come from a single gluon line [30].

The total cross section for charm production in the next-to-leading order in QCD has been previously derived. In the present study, we use the results given in Refs. [31] and [30], where the soft divergences in the next-order $2 \to 3$ processes are eliminated by corresponding divergences in virtual corrections to the leading-order $2 \to 2$ processes, while the ultraviolet divergences in virtual corrections are handled by renormalization in the modified minimal-subtraction ($\overline{MS}$) scheme [32,33]. Choosing the QCD running coupling constant as $\alpha_s(m_c)$ and the renormalization scale as the charm quark mass, we have calculated the cross sections for the production of charm pairs with charm quark mass $m_c = 1.3$ GeV from massless light quarks and gluons, and they are shown in Fig. 1 as functions of center-of-mass energy for the quark-antiquark annihilation (left panel) and gluon-gluon fusion (right panel) processes. The dashed and solid lines correspond to results for the leading order and the next-to-leading order, respectively. It can be seen that for charm production from quark-antiquark annihilation, the next-to-leading order gives a larger cross section at low energies but a smaller one at high energies. On the other hand, the cross section for charm production from gluon-gluon fusion in the next-to-leading order is significantly larger than that in the leading order at all energies.

B. Thermal averaged charm production cross sections

In the kinetic model to be used in the next section for studying charm quark production and annihilation in a quark-gluon plasma, thermal averaged cross sections are needed. In terms of the thermal distribution functions $f_i(\mathbf{p})$ of quarks and gluons in the quark-gluon plasma and the relative velocity v_{ab} of two initial interacting partons a and b, the thermal averaged cross section $\sigma_{ab\to cd}$ for the reaction $ab \to cd$ is given by [34]

$$\begin{aligned} \langle \sigma_{ab\to cd} v \rangle &= \frac{\int d^3\mathbf{p}_a d^3\mathbf{p}_b f_a(\mathbf{p}_a) f_b(\mathbf{p}_b) \sigma_{ab\to cd} v_{ab}}{\int d^3\mathbf{p}_a d^3\mathbf{p}_b f_a(\mathbf{p}_a) f_b(\mathbf{p}_b)} \\ &= \left[4\alpha_a^2 K_2(\alpha_a)\alpha_b^2 K_2(\alpha_b)\right]^{-1} \\ &\quad \times \int_{z_0}^{\infty} dz [z^2 - (\alpha_a + \alpha_b)^2][z^2 - (\alpha_a - \alpha_b)^2] \\ &\quad \times K_1(z)\sigma(s = z^2 T^2), \end{aligned} \tag{6}$$

with $\alpha_i = m_i/T$, $z_0 = \max(\alpha_a + \alpha_b, \alpha_c + \alpha_d)$, and K_1 being the modified Bessel function.

In the quark-gluon plasma, quarks and gluons acquire thermal masses. As an exploratory study, we include this effect

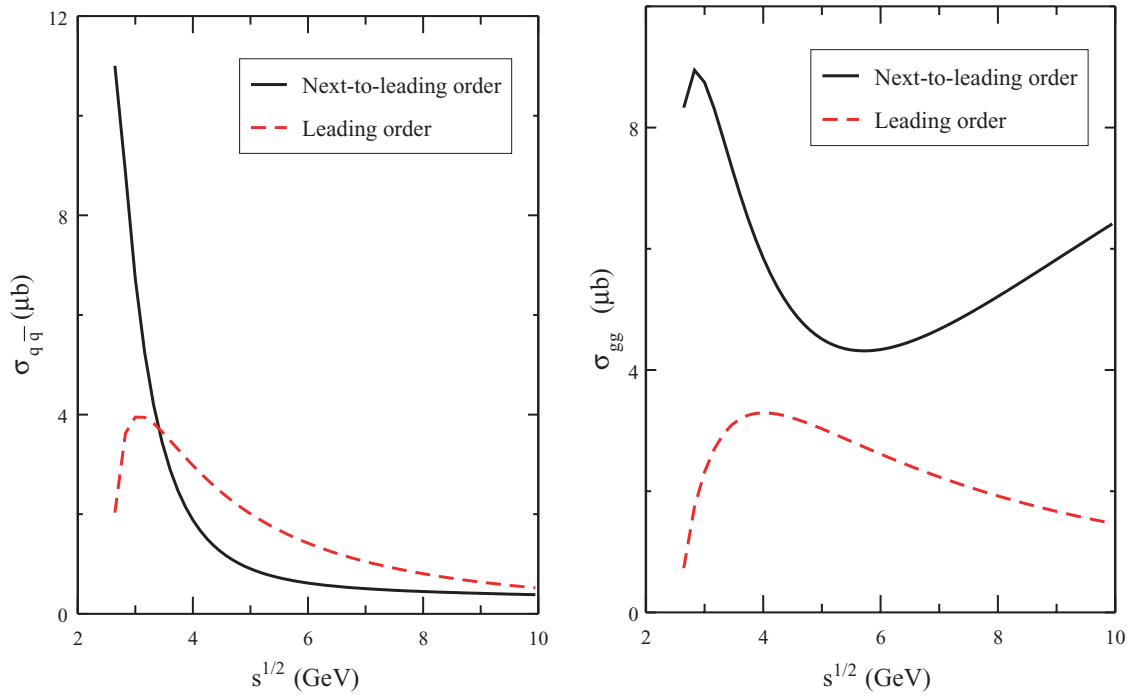

FIG. 1. (Color online) Charm quark pair production cross sections as functions of center-of-mass energy from quark-antiquark annihilation (left panel) and gluon-gluon fusion (right panel) in both the leading (dashed line) and the next-to-leading (solid line) order. The charm quark mass is taken to be $m_c = 1.3\,\text{GeV}$, while light quarks and gluons are massless.

in their distribution functions but not in the calculation of their scattering cross sections. For the thermal masses of quarks and gluons, they are taken to be [35,36]

$$m_q = gT/\sqrt{6} \quad \text{and} \quad m_g = gT/\sqrt{2}, \tag{7}$$

where g is the QCD coupling constant and is taken to have the value $g = \sqrt{4\pi\alpha_s(2\pi T)}$. With the charm quark mass $m_c = 1.3\,\text{GeV}$, the thermal averaged cross section for charm production in a quark-gluon plasma is shown in Fig. 2 as a functions of the temperature of the quark-gluon plasma for quark-antiquark annihilation (left panel) and gluon-gluon fusion (right panel). For both reactions, thermal averaged cross sections in the next-to-leading order (solid line) are significantly larger than those in the leading order (dashed line).

III. CHARM PRODUCTION IN HEAVY ION COLLISIONS AT LHC

Using the thermal averaged charm production cross sections described above, we study in this section the time evolution of the abundance of charm quark pairs in heavy ion collisions at LHC using a kinetic model based on the rate equation that takes into account both production and annihilation of charm quarks in the produced quark-gluon plasma. For the dynamics of the quark-gluon plasma, we describe it by a schematic hydrodynamic model and assume that both quarks and gluons are in thermal and chemical equilibrium during the evolution. We further assume that all produced charm quarks including those produced directly from the initial hard collisions are also in thermal equilibrium, although not in chemical equilibrium. The latter is consistent with observed large elliptic flow of the electrons from charmed meson decays in heavy ion collisions at RHIC [37,38], which requires that charm quarks interact strongly in the quark-gluon plasma and thus are likely to reach thermal equilibrium [39–41].

A. The rate equation

The time evolution of the number density of charm quark pairs $n_{c\bar{c}}$ in an expanding quark-gluon plasma can be described by the rate equation [42,43]

$$\begin{aligned}\partial_\mu(n_{c\bar{c}}u^\mu) = {} & R_{q\bar{q}\to c\bar{c}} + R_{q\bar{q}\to c\bar{c}g} + R_{gg\to c\bar{c}} + R_{gg\to c\bar{c}g} \\ & - R_{c\bar{c}\to q\bar{q}} - R_{c\bar{c}g\to q\bar{q}} - R_{c\bar{c}\to gg} - R_{c\bar{c}g\to gg}.\end{aligned} \tag{8}$$

In the above equation, $u^\mu = \gamma(1, \mathbf{v})$ is the four velocity of a fluid element in the quark-gluon plasma with velocity $\mathbf{v}$ and the corresponding Lorentz factor γ, and the terms on the left-hand side of above equation are the charm pair production and annihilation rates. For the next-to-leading order, the charm pair production rate is given by

$$\begin{aligned} R_{q\bar{q}\to c\bar{c}} &= \langle\sigma_{q\bar{q}\to c\bar{c}}v\rangle n_q n_{\bar{q}}, \\ R_{gg\to c\bar{c}} &= \frac{1}{2}\langle\sigma_{gg\to c\bar{c}}v\rangle n_g^2, \\ R_{q\bar{q}\to c\bar{c}g} &= \langle\sigma_{q\bar{q}\to c\bar{c}g}v\rangle n_q n_{\bar{q}}, \\ R_{gg\to c\bar{c}g} &= \frac{1}{2}\langle\sigma_{gg\to c\bar{c}g}v\rangle n_g^2, \end{aligned} \tag{9}$$

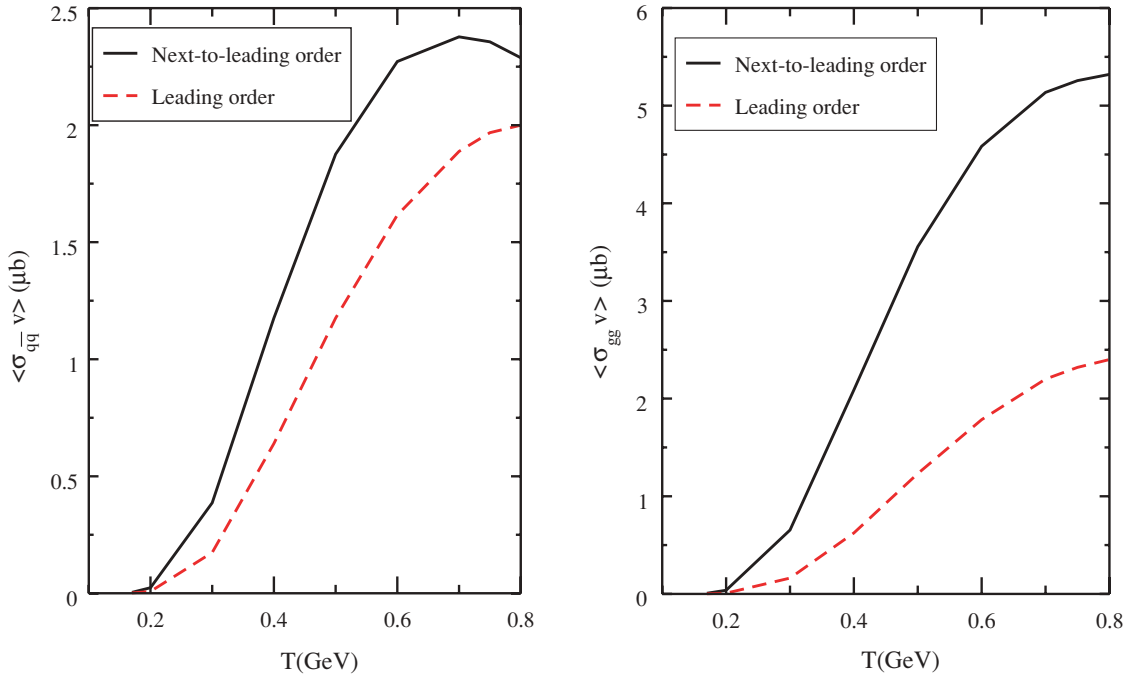

FIG. 2. (Color online) Thermal averaged cross sections for charm pair production from quark-antiquark annihilation (left panel) and gluon-gluon fusion (right panel) in a quark-gluon plasma as functions of temperature. The charm quark mass is taken to be $m_c = 1.3\,\text{GeV}$ while quarks and gluons are taken to have thermal masses given by Eq. (7).

where n_g, n_q, and $n_{\bar{q}}$ denote the gluon, quark, and antiquark densities in the quark-gluon plasma, respectively, and they are taken to have their equilibrium values. The leading-order cross sections $\sigma_{q\bar{q}\to c\bar{c}}$ and $\sigma_{g\bar{g}\to c\bar{c}}$ in above equation are computed from the processes in Eq. (1), while the cross sections $\sigma_{q\bar{q}\to c\bar{c}g}$ and $\sigma_{g\bar{g}\to c\bar{c}g}$ for the next-order $2 \to 3$ processes include both the processes in Eq. (3) and the virtual corrections to the leading-order processes.

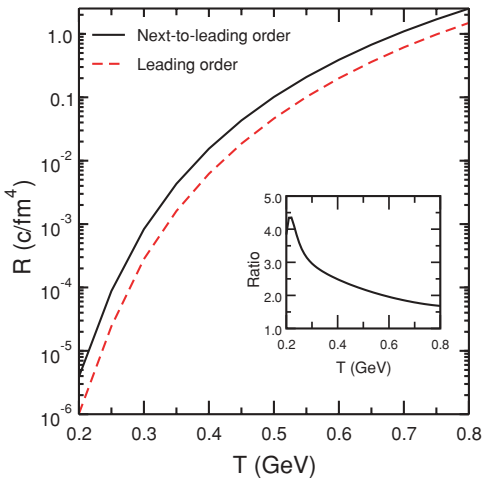

FIG. 3. (Color online) Thermal charm quark production rate as a function of temperature for massive partons and charm quark mass $m_c = 1.3\,\text{GeV}$. The inset gives the ratio of the charm production rate in the next-to-leading order to that in the leading order.

In Fig. 3, we show the thermal charm production rate as a function of temperature with massive quarks and gluons in a thermally and chemically equilibrated quark-gluon plasma. It can be seen that the charm production rate increases almost exponentially with increasing temperature. With the initial temperature $T_0 \simeq 350$ MeV in central heavy ion collisions at RHIC, the thermal charm production rate is more than two orders of magnitude smaller than that at the temperature $T_0 \simeq 700$ MeV expected to be reached in central heavy ion collisions at LHC. This thus justifies the neglect of thermal charm production at RHIC. The inset in Fig. 3 gives the ratio of the charm production rate in the next-to-leading order to that in the leading order, which is seen to vary from ∼4.5 at low temperatures to ∼1.8 at high temperatures.

Because the charm pair annihilation rate and production rate become equal when the charm quark abundance reaches chemical equilibrium, i.e.,

$$\begin{aligned} R^{\text{eq}}_{c\bar{c}\to q\bar{q}} &= R^{\text{eq}}_{q\bar{q}\to c\bar{c}} = \langle\sigma_{q\bar{q}\to c\bar{c}}v\rangle n^{\text{eq}}_q n^{\text{eq}}_{\bar{q}}, \\ R^{\text{eq}}_{c\bar{c}\to gg} &= R^{\text{eq}}_{gg\to c\bar{c}} = \frac{1}{2}\langle\sigma_{gg\to c\bar{c}}v\rangle\left(n^{\text{eq}}_g\right)^2, \\ R^{\text{eq}}_{c\bar{c}g\to q\bar{q}} &= R^{\text{eq}}_{q\bar{q}\to c\bar{c}g} = \langle\sigma_{q\bar{q}\to c\bar{c}g}v\rangle n^{\text{eq}}_q n^{\text{eq}}_{\bar{q}}, \\ R^{\text{eq}}_{c\bar{c}g\to gg} &= R^{\text{eq}}_{gg\to c\bar{c}g} = \frac{1}{2}\langle\sigma_{gg\to c\bar{c}g}v\rangle\left(n^{\text{eq}}_g\right)^2, \end{aligned} \tag{10}$$

where n^{eq} is the equilibrium density while R^{eq} is the rate evaluated with the equilibrium densities, the charm pair annihilation rates in the leading order and the next-to-leading

order can thus be written as

$$\begin{aligned} R_{c\bar{c}\to q\bar{q}} &= \langle\sigma_{q\bar{q}\to c\bar{c}}v\rangle\left(n_q^{\rm eq}\right)^2\left(\frac{n_{c\bar{c}}}{n_{c\bar{c}}^{\rm eq}}\right)^2, \\ R_{c\bar{c}\to gg} &= \frac{1}{2}\langle\sigma_{gg\to c\bar{c}}v\rangle\left(n_g^{\rm eq}\right)^2\left(\frac{n_{c\bar{c}}}{n_{c\bar{c}}^{\rm eq}}\right)^2, \\ R_{c\bar{c}g\to q\bar{q}} &= \langle\sigma_{q\bar{q}\to c\bar{c}g}v\rangle\left(n_q^{\rm eq}\right)^2\left(\frac{n_{c\bar{c}}}{n_{c\bar{c}}^{\rm eq}}\right)^2, \\ R_{c\bar{c}g\to gg} &= \frac{1}{2}\langle\sigma_{gg\to c\bar{c}g}v\rangle\left(n_g^{\rm eq}\right)^2\left(\frac{n_{c\bar{c}}}{n_{c\bar{c}}^{\rm eq}}\right)^2. \end{aligned} \tag{11}$$

In the above equations, we have assumed that the density of quarks is the same as that of antiquarks, i.e., $n_q^{\rm eq} = n_{\bar{q}}^{\rm eq}$.

With the above equations and taking light quarks and gluons to be in thermal and chemical equilibrium, the rate equation Eq. (8) can be rewritten as

$$\begin{aligned} \partial_\mu(n_{c\bar{c}}u^\mu) = &\Big[(\langle\sigma_{q\bar{q}\to c\bar{c}}v\rangle + \langle\sigma_{q\bar{q}\to c\bar{c}g}v\rangle)\left(n_q^{\rm eq}\right)^2 \\ &+ \frac{1}{2}(\langle\sigma_{gg\to c\bar{c}}v\rangle + \langle\sigma_{gg\to c\bar{c}g}v\rangle)\left(n_g^{\rm eq}\right)^2\Big] \\ &\times\left[1 - \left(\frac{n_c}{n_c^{\rm eq}}\right)^2\right]. \end{aligned} \tag{12}$$

B. Collision dynamics at LHC

In central heavy ion collisions at RHIC, the particle distribution at midrapidity is approximately uniform, so the Bjorken boost-invariant hydrodynamic solution is a good approximation for describing the time evolution of the hot dense matter formed in these collisions [44]. Such a model indeed gives a good description of the experimental data at RHIC [45]. Also, recent studies based on the AdS/CFT correspondence have demonstrated that at late proper times the system produced in relativistic heavy ion collisions in the strongly coupled regime described by gauge-gravity duality exhibits an energy density scaling with characteristics similar to those of the Bjorken hydrodynamic solution [46,47]. We thus expect that the longitudinal dynamics in heavy ion collisions at LHC is also boost invariant. To include the effect of transverse flow, we further include an accelerated transverse expansion, resulting in a cylindrical symmetry in the geometry of the collision. In terms of the cylindrical coordinates r and φ as well as the proper time τ and the space-time rapidity η defined by [42,43]

$$\tau = \sqrt{t^2 - z^2}, \quad \eta = \frac{1}{2}\ln\frac{t+z}{t-z}, \tag{13}$$

we then have $u^\eta = u^\varphi = 0$. If we further assume a uniform density distribution in the transverse plane and take the average over the radial coordinate, the left-hand side of the rate equation Eq. (12) can then be expressed as

$$\frac{1}{\tau R^2(\tau)}\frac{\partial}{\partial\tau}(\tau R^2(\tau)n_{c\bar{c}}\langle u^\tau\rangle), \tag{14}$$

where $R(\tau)$ denotes the transverse radius of the system, and $\langle u^\tau\rangle$ is the averaged τ component of the four velocity defined as

$$\langle u^\tau\rangle = \frac{2}{R^2(\tau)}\int_0^{R(\tau)} dr\, r u^\tau(r). \tag{15}$$

At midrapidity, the four velocity of a fluid element u^μ can be described by two independent boosts in longitudinal and radial directions [48], with the radial flow velocity β_r given by

$$u^\tau = \gamma_r = \frac{1}{\sqrt{1-\beta_r^2}}. \tag{16}$$

Assuming the usual ansatz for the radial expansion velocity [42,43,48,49]

$$\beta_r(\tau, r) = \frac{dR}{d\tau}\left(\frac{r}{R}\right), \tag{17}$$

we have

$$\langle u^\tau\rangle = \int_0^1 dy\,\frac{1}{\sqrt{1-(dR/d\tau)^2 y}}. \tag{18}$$

With the time evolution of the transverse radius of the fire cylinder taken to be [50]

$$R(\tau) = R_0 + a(\tau - \tau_0)^2/2, \tag{19}$$

where R_0 and τ_0 are the initial radius and proper time of the fire cylinder, respectively, and a denotes the transverse acceleration, the volume of the fireball at proper time τ is then given by

$$V(\tau) = \pi R^2(\tau)\tau. \tag{20}$$

In the following, we choose the initial transverse radius of the fire cylinder to be the radius of the colliding Pb nucleus, i.e., $R_0 = 7.0\,$fm, and a transverse acceleration $a = 0.1\,c^2/$fm to obtain a reasonable final transverse flow velocity.

C. Time evolution of the temperature of the quark-gluon plasma

To estimate the initial temperature of produced quark-gluon plasma, we use two different models: a multiphase transport (AMPT) model [51] and a model based on the color glass condensate (CGC) [52]. Using the AMPT model, we obtain an initial transverse energy of about 3000 GeV per unit rapidity at the midrapidity in central Pb + Pb collisions at $\sqrt{s_{NN}} = 5.5\,$TeV. Most of this initial energy is concentrated within a transverse radius of about 4.7 fm that is smaller than the radius of the colliding nuclei as a result of their surface diffuseness. If we take an initial proper time of $\tau_0 = 0.2\,{\rm fm}/c$, earlier than that at RHIC, the initial energy density of produced quark-gluon plasma is then about

$$\epsilon_0 \approx \frac{dE_T/dy}{\pi R_0^2\tau_0} \approx \frac{3000}{\pi\times 4.7^2\times 0.2} \approx 226\,{\rm GeV/fm^3}. \tag{21}$$

Using the relation

$$\epsilon = \frac{37\pi^2 T^4}{30} \approx (T/160\,{\rm MeV})^4\,{\rm GeV/fm^3} \tag{22}$$

for the energy density of a quark-gluon plasma with massless quarks and gluons, the initial temperature of the quark-gluon

plasma formed at LHC is thus $T_0 \approx 620$ MeV. This number turns out to be very close to that predicted by the CGC model. As shown in Ref. [52], the glasma formed after Pb + Pb collisions at $\sqrt{s_{NN}} = 5.5$ TeV has an energy density of about $\epsilon \sim 700\,\mathrm{GeV/fm^3}$ at a proper time $\tau \sim 0.07\,\mathrm{fm}/c$. The glasma then evolves into a thermalized quark-gluon plasma at a proper time τ_0. Assuming that the energy density decreases inversely with the proper time during this stage, its value at $\tau_0 \sim 0.2\,\mathrm{fm}/c$ is then $\epsilon_0 \approx 245\,\mathrm{GeV/fm^3}$, corresponding to an initial temperature $T_0 \approx 633$ MeV. Because the result from the CGC model depends on the fourth power of the saturation momentum, the predicted initial temperature thus has a large uncertainty. The same is true for the AMPT model as the predicted total transverse energy is sensitive to the parton structure function of the nucleon, the initial nuclear shadowing, and the saturation of produced gluons. Therefore, we consider in the following also a scenario with an initial energy density that is 50% or a factor of two larger larger than above value, corresponding to an initial temperature of about 700 or 750 MeV, respectively.

We note for central Au + Au collisions at $\sqrt{s_{NN}} =$ 200 GeV at RHIC, the total transverse energy from the AMPT model is about 1000 GeV. Taking a proper time $\tau_0 = 0.5\,\mathrm{fm}/c$ for the formation of an equilibrated quark-gluon plasma as required by the hydrodynamic model to explain the observed hadron elliptic flows [53–55], the initial energy density and temperature of produced quark-gluon plasma are then $\epsilon_0 \approx 33\,\mathrm{GeV/fm^3}$ and $T_0 \approx 383$ MeV, respectively. These values are again similar to those from the CGC model, which gives an energy density $\epsilon \approx 130\,\mathrm{GeV/fm^3}$ at $\tau_0 = 0.1\,\mathrm{fm}/c$, leading thus to $\epsilon_0 \approx 26\,\mathrm{GeV/fm^3}$ and $T_0 \approx 361$ MeV at $\tau_0 = 0.5\,\mathrm{fm}/c$. With such a low initial temperature, charm production from the quark-gluon plasma is thus negligible according to the production rates shown in Fig. 3.

For the time evolution of the temperature of produced quark-gluon plasma at LHC, we determine it using the entropy conservation, and the results are shown in Fig. 4 for the three initial temperatures $T_0 = 630$, 700, and 750 MeV. In all cases, the critical temperature for the quark-gluon plasma phase transition to the hadronic matter is taken to be $T_C = 170$ MeV. It can be seen that the temperature decreases very quickly with the proper time for all three initial temperatures, dropping below 400 MeV after about 0.5, 1, and 1.5 fm/c for $T_0 = 630$, 700, and 750 MeV, respectively.

IV. RESULTS

For central Pb + Pb collisions at $\sqrt{s_{NN}} = 5.5$ TeV at LHC ,the number of charm pairs produced in one unit rapidity from initial hard nucleon-nucleon collisions is about 20 at midrapidity according to the next-to-leading order pQCD calculations [12]. Neglecting the contribution from prethermal production, we solve the rate equation with this initial number of charm quark pairs and certain initial temperature and proper time for the produced quark-gluon plasma. We vary the initial temperature and proper time to study their effects on the final number of charm quark pairs produced in these collisions.

We first consider the case of an initial temperature $T_0 =$ 700 MeV and proper time $\tau_0 = 0.2\,\mathrm{fm}/c$. For the charm quark mass, we take it to be $m_c = 1.3$ GeV as that extracted from the experimental data in e^+e^- and pp collisions. To take into account the medium effect on quarks and gluons, we use the thermal masses given in Eq. (7). The time evolution of the total number of charm quark pairs obtained from these initial conditions in central Pb + Pb collisions at $\sqrt{s_{NN}} = 5.5$ TeV is shown in Fig. 5. It can be seen that including thermal production enhances the total number of final charm pairs as compared to that from initial direct production. The charm pair number reaches the peak value at $\tau \sim 2$ fm/c and then deceases with the proper time. At the critical temperature $T_C = 170$ MeV when the proper time is $\tau_C \approx 6.4$ fm/c, the number of charm pairs is about 27 in the next-to-leading order (solid line), which is about 30% larger than the number due to

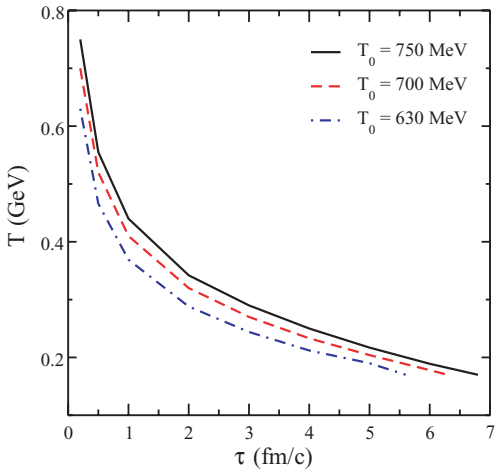

FIG. 4. (Color online) Time evolution of the temperature of the quark-gluon plasma formed in Pb + Pb collisions at $\sqrt{s_{NN}} = 5.5$ TeV for different initial temperatures and the same initial proper time $\tau_0 = 0.2\,\mathrm{fm}/c$.

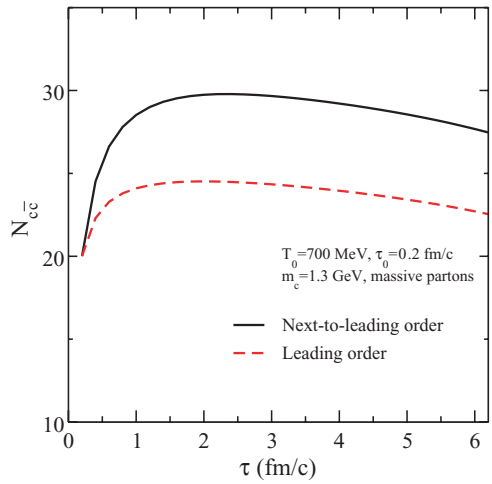

FIG. 5. (Color online) Number of charm pairs as a function of proper time in central Pb + Pb collisions at $\sqrt{s_{NN}} = 5.5$ TeV in the leading order (dashed line) and the next-to-leading order (solid line) in QCD.

direct production from initial hard collisions. The final charm pair number is reduced to about 22 if only thermal production from the leading-order contribution is included as shown by the dashed line.

We note that the final charm quark pair number is much larger than its chemical equilibrium value at $T_C = 170$ MeV, which is about 4.7. This is not surprising as the time for charm pairs to reach their equilibrium number $n_c^{\rm eq}$ at certain temperature, given by $\tau_{\rm eq} = n_{c\bar{c}}^{\rm eq}/2R_{c\bar{c}}$, with $R_{c\bar{c}}$ denoting the production rate at that temperature, increases dramatically with decreasing quark-gluon plasma temperature from a value of a few fm/c at $T = 700$ MeV to a few thousands of fm/c at $T_c = 170$ MeV. It is thus not possible for charm quarks to reach chemical equilibrium during the finite lifetime of the produced quark-gluon plasma at LHC. Because the initial number of charm quark pairs produced from hard scattering of initial nucleons is large at LHC and the charm production rate is also larger during the early stage of the quark-gluon plasma when its temperature is high, there are more charm pairs in the quark-gluon plasma than the equilibrium number at the critical temperature. As the quark-gluon plasma expands and cools, the charm annihilation rate decreases, making it less likely to destroy the produced charm pairs and leading thus to an oversaturation of the charm abundance at the critical temperature.

Because there is substantial uncertainty in the charm quark pairs produced from initial direct production [12,14], we have also studied thermal charm production using different initial charm quark pair numbers. Varying the initial charm pair number by a factor of two, we have repeated the above calculations, and the results based on the next-to-leading order in QCD are shown in Fig. 6. For initial numbers of charm quark pairs of 10, 20, and 40, the final numbers are found to be about 19, 27, and 45, respectively. Thermal production of charm quarks from the quark-gluon plasma thus becomes more important as the initial charm pair number becomes smaller.

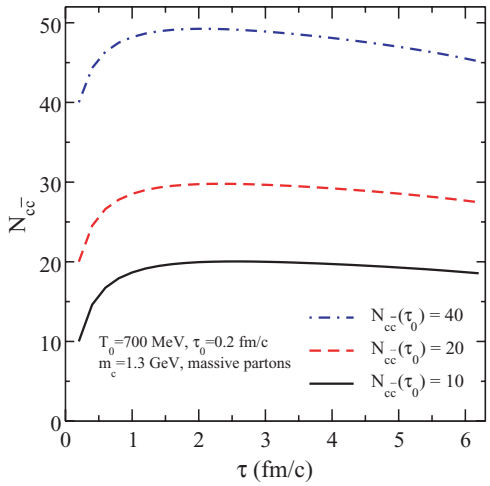

FIG. 6. (Color online) Number of charm pairs as a function of proper time in central Pb + Pb collisions at $\sqrt{s_{NN}} = 5.5$ TeV for different numbers of charm quark pairs produced from initial hard scattering.

Returning to the case of 20 initial charm quark pairs, we note that in the above calculations, we used massive quarks and gluons given by the thermal QCD calculations. To see how these masses affect thermal charm production, we carried out calculations similar to those above with massless quarks and gluons but with the same initial conditions of $T_0 = 700$ MeV and $\tau_0 = 0.2$ fm/c as well as the charm quark mass of $m_c = 1.3$ GeV. We found that the resulting number of charm quark pairs at $T_C = 170$ MeV hardly differs from the massive case. The reason for this is that although using massless quarks and gluons reduces the thermal averaged charm production cross sections, the effect is largely compensated by the larger quark and gluon densities if they are massless.

As previously mentioned, the charm production rate exhibits an exponential increase with the temperature of the quark-gluon plasma. The total number of charm quark pairs produced in heavy ion collisions thus depends on the initial temperature of the expanding quark-gluon plasma. In Fig. 7, we show the total number of charm pairs as a function of proper time in central Pb + Pb collisions at $\sqrt{s_{NN}} = 5.5$ TeV for different initial temperatures of the quark-gluon plasma but the same initial proper time $\tau_0 = 0.2$ fm/c. It can be seen that the final number of charm quark pairs at the critical temperature $T_C = 170$ MeV calculated in the next-to-leading order decreases to about 22 for $T_0 = 630$ MeV and increases to about 33 for $T_0 = 750$ MeV.

We have also considered the effect of the initial proper time on thermal charm production by using $\tau_0 = 0.5$ fm/c as that in heavy ion collisions at RHIC. The predicted initial temperature from the CGC model is then $T_0 = 500$ MeV. Results for this initial temperature as well as those for the temperatures of 560 and 600 MeV, which correspond, respectively, to an increase of the initial energy by 50 and 100% of that for $T_0 = 500$ MeV, show that the final total number of charm quark pairs is only slightly reduced compared to that for an initial proper time $\tau_0 = 0.2$ fm/c, i.e., 21, 26, and 32 for the above three temperatures.

The charm quark mass also affects the contribution of thermal charm production. With $m_c = 1.5$ GeV and the initial proper time $\tau_0 = 0.2$ fm/c, the final total number of charm

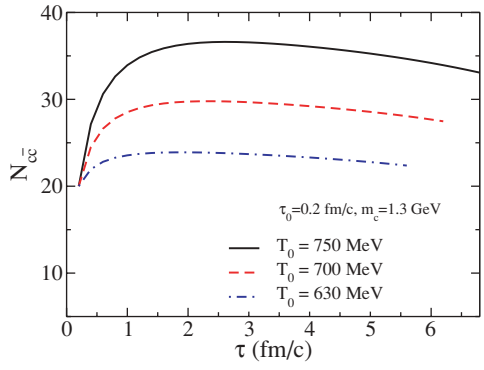

FIG. 7. (Color online) Total number of charm pairs as a function of proper time in central Pb + Pb collisions at $\sqrt{s_{NN}} = 5.5$ TeV for different initial temperatures of the quark-gluon plasma but the same initial proper time $\tau_0 = 0.2$ fm/c.

quark pairs is reduced to about 20, 22, and 25 for the three initial temperatures $T_0 = 630$, 700, and 750 MeV, respectively.

V. SUMMARY AND DISCUSSIONS

In this article, we carried out the first calculation of thermal charm production at next-to-leading order in QCD. Modeling central heavy ion collisions at LHC by a schematic longitudinally boost invariant and transversely expanding fire cylinder of quark-gluon plasma, we evaluated the number of charm quark pairs produced in these collisions. With an initial temperature of 700 MeV for an equilibrated quark-gluon plasma at an initial proper time of 0.2 fm/c and a charm quark mass of 1.3 GeV, we obtained about 30% enhancement in the production of charm quarks over that produced directly from initial hard collisions, if the latter is taken to be 20 pairs at midrapidity according to the next-to-leading order pQCD calculations. About equal contributions were obtained from the leading-order $2 \to 2$ and the next-order $2 \to 3$ processes. This result is, however, sensitive to the initial conditions for the produced quark-gluon plasma as well as the charm quark mass. The enhancement is increased to about 80% if the initial temperature is increased to 750 MeV but reduced to about 10% if the initial temperature is decreased to 630 MeV. Delaying the proper time at which a thermalized quark-gluon plasma is formed does not affect, however, much thermal charm quark production because the effect due to decreased initial temperature is compensated by that from the increased volume of the quark-gluon plasma. Changing the charm quark mass has, on the other hand, a large effect on thermal charm quark production from the quark-gluon plasma. With a larger charm quark mass of $m_c = 1.5$ GeV, thermal charm quark production from the quark-gluon plasma becomes unimportant even for an initial temperature of $T_0 = 700$ MeV. Finally, thermal charm production from the quark-gluon plasma becomes more important if the number of directly produced charm pairs from initial hard scattering is small. These results are of interest not only in their own right but also because they are useful for understanding charmonium production in relativistic heavy ion collisions because its production from the quark-gluon plasma is proportional to the square of the charm quark numbers.

ACKNOWLEDGMENTS

This work was supported in part by the U.S. National Science Foundation under Grant PHY-0457265 and the Welch Foundation under Grant A-1358. Ben-Wei Zhang was further supported by the National Natural Science Foundation of China under Project 10405011 and by MOE of China under Project IRT0624.

[1] I. Arsene *et al.* (BRAHMS Collaboration), Nucl. Phys. **A757**, 1 (2005).
[2] B. B. Back *et al.* (PHOBOS Collaboration), Nucl. Phys. **A757**, 28 (2005).
[3] J. Adams *et al.* (STAR Collaboration), Nucl. Phys. **A757**, 102 (2005).
[4] K. Adcox *et al.* (PHENIX Collaboration), Nucl. Phys. **A757**, 184 (2005).
[5] T. Matsui and H. Satz, Phys. Lett. **B178**, 416 (1986).
[6] M. Asakawa and T. Hatsuda, Phys. Rev. Lett. **92**, 012001 (2004).
[7] S. Datta, F. Karsch, P. Petreczky, and I. Wetzorke, Phys. Rev. D **69**, 094507 (2004).
[8] B. Zhang, C. M. Ko, B. A. Li, Z. W. Lin, and B. H. Sa, Phys. Rev. C **62**, 054905 (2000); B. Zhang, C. M. Ko, B. A. Li, Z. W. Lin, and S. Pal, *ibid.* **65**, 054909 (2002).
[9] H. Satz, J. Phys. G **32**, R25 (2006).
[10] L. Grandchamp, S. Lumpkins, D. Sun, H. van Hees, and R. Rapp, Phys. Rev. C **73**, 064906 (2006).
[11] R. L. Thews and M. L. Mangano, Phys. Rev. C **73**, 014904 (2006).
[12] A. Andronic, P. Braun-Munzinger, K. Redlich, and J. Stachel, Phys. Lett. **B571**, 36 (2003).
[13] V. Greco, C. M. Ko, and R. Rapp, Phys. Lett. **B595**, 202 (2004).
[14] S. Gavin, P. L. McGaughey, P. V. Ruuskanen, and R. Vogt, Phys. Rev. C **54**, 2606 (1996).
[15] R. Vogt, J. Phys. G **31**, S773 (2005).
[16] A. Adare *et al.* (PHENIX Collaboration), Phys. Rev. Lett. **97**, 252002 (2006).
[17] J. Adams *et al.* (STAR Collaboration), Phys. Rev. Lett. **94**, 062301 (2005).
[18] Z. W. Lin and M. Gyulassy, Phys. Rev. C **51**, 2177 (1995).
[19] P. Lévai, B. Muller, and X. N. Wang, Phys. Rev. C **51**, 3326 (1995).
[20] T. Matsui, B. Svetitsky, and L. D. McLerran, Phys. Rev. D **34**, 783 (1986).
[21] T. S. Biro, P. Lévai, and B. Muller, Phys. Rev. D **42**, 3078 (1990).
[22] P. Levai and R. Vogt, Phys. Rev. C **56**, 2707 (1997).
[23] B. Kämpfer and O. P. Pavlenko, Phys. Lett. **B391**, 185 (1997).
[24] W. Cassing, L. A. Kondratyuk, G. I. Lykasove, and M. V. Rzjanin, Phys. Lett. **B513**, 1 (2001).
[25] W. Liu and C. M. Ko, Phys. Lett. **B533**, 259 (2002).
[26] W. Liu, C. M. Ko, and S. H. Lee, Nucl. Phys. **A728**, 457 (2003).
[27] W. Cassing, E. L. Bratkovskaya, and A. Sibirtsev, Nucl. Phys. **A691**, 753 (2001).
[28] J. Letessier and J. Rafelski, Phys. Rev. C **75**, 014905 (2007).
[29] J. Letessier and J. Rafelski, *Hadrons and Quark-Gluon Plasma* (Cambridge University Press, Cambridge, UK, 2002), Chap. 17.
[30] P. Nason, S. Dawson, and R. K. Ellis, Nucl. Phys. **B303**, 607 (1988); **B327**, 49 (1989).
[31] W. Beenakker, H. Kuijf, W. L. van Neerven, and J. Smith, Phys. Rev. D **40**, 54 (1989); W. Beenakker, W. L. van Neerven, R. Meng, G. A. Schuler, and J. Smith, Nucl. Phys. **B351**, 507 (1991).
[32] R. D. Field, *Applications of Perturbative QCD* (Addison-Wesley, Reading, MA, 1989), Chaps. 2 and 6.
[33] M. E. Peskin and D. V. Schroeder, *An Introduction to Quantuam Field Theory* (Addison–Wesley Advanced Book Program, Reading, MA, 1995), Chap. 17.
[34] C. M. Ko, X. N. Wang, B. Zhang, and X. F. Zhang, Phys. Lett. **B444**, 237 (1998).
[35] M. Le Bellac, *Thermal Field Theory* (Cambridge University Press, Cambridge, UK, 1996), Chaps. 6 and 7.
[36] J. P. Blaizot and E. Iancu, Phys. Rep. **359**, 355 (2002).

[37] S. S. Adler *et al*. (PHENIX Collaboration), Phys. Rev. C **72**, 024901 (2005).
[38] F. Laue (STAR Collaboration), J. Phys. G **31**, S27 (2005).
[39] H. van Hees and R. Rapp, Phys. Rev. C **71**, 034907 (2005).
[40] B. Zhang, L. W. Chen, and C. M. Ko, Phys. Rev. C **72**, 024906 (2005); Nucl. Phys. **A774**, 665 (2006).
[41] D. Molnar, J. Phys. G **31**, S421 (2005).
[42] C. M. Ko and L. Xia, Phys. Rev. C **38**, 179 (1988); Z. W. Lin and C. M. Ko, *ibid*. **62**, 034903 (2000); W. Liu and C. M. Ko, Nucl. Phys. **A765**, 401 (2006).
[43] L. Alvarez-Ruso and V. Koch, Phys. Rev. C **65**, 054901 (2002).
[44] J. D. Bjorken, Phys. Rev. D **27**, 140 (1983).
[45] P. F. Kolb and U. W. Heinz, in *Quark-Gluon Plasma 3*, edited by R. C. Hwa and X. N. Wang (World Scientific, Singapore, 2003).
[46] R. A. Janik and R. Peschanski, Phys. Rev. D **73**, 045013 (2006).
[47] Y. V. Kovchegov and A. Taliotis, arXiv:0705.1234[hep-ph].
[48] E. Schnedermann, J. Sollfrank, and U. Heinz, Phys. Rev. C **48**, 2462 (1993).
[49] J. P. Bondorf, S. I. A. Garpman, and J. Zimanyi, Nucl. Phys. **A296**, 320 (1978).
[50] L. W. Chen, V. Greco, C. M. Ko, S. H. Lee, and W. Liu, Phys. Lett. **B601**, 34 (2004).
[51] B. Zhang, C. M. Ko, B. A. Li, and Z. W. Lin, Phys. Rev. C **61**, 067901 (2000); Z. W. Lin, C. M. Ko, B. A. Li, B. Zhang, and S. Pal, *ibid*. **72**, 064901 (2005).
[52] T. Lappi, Phys. Lett. **B643**, 11 (2006).
[53] D. Teaney, J. Lauret, and E. V. Shuryak, Phys. Rev. Lett. **86**, 4783 (2001).
[54] P. Huovinen, P. F. Kolb, and U. Heinz, Nucl. Phys. **A698**, 475 (2002).
[55] T. Hirano and K. Tsuda, Phys. Rev. C **66**, 054905 (2002).